Biophysical Chemistry 16 (1982) 223–240
Elsevier Biomedical Press

DIFFERENTIAL-WAVELENGTH DECONVOLUTION OF TIME-RESOLVED FLUORESCENCE INTENSITIES

A NEW METHOD FOR THE ANALYSIS OF EXCITED-STATE PROCESSES

Joseph R. LAKOWICZ and Aleksander BALTER

Department of Biological Chemistry, University of Maryland, School of Medicine, 660 West Redwood Street, Baltimore, MD 21201, U.S.A.

Received 10th June 1982
Accepted 10th June 1982

Key words: Differential-wavelength devonvolution; Excited-state process; Fluorescence decay

We describe a new procedure for the analysis of time-resolved decays of fluorescence intensity observed for excited-state reactions. This procedure is particularly valuable because it simplifies both determination of the rate constants of excited-state reactions and calculation of the emission spectra of the unreacted and the reacted species. These advantages are obtained without additional data acquisition, by the further analysis of data which would already be collected. As is usual for an excited-state process, time-resolved decays of fluorescence intensity are collected at wavelengths across the emission spectrum. Generally, one derives analytical expressions for the impulse response by deconvolution using the time profile of the exciting pulse. We suggest that in addition to the procedure just described, the response observed at longer wavelengths be deconvolved using the response observed on the blue side of the emission. Typically, this emission is from the initially excited state of the fluorophore (F). Then, the derived decay time is the decay rate of the reacted species (R). In addition, spectral overlap of the F and R states is revealed quantitatively as an apparent zero-decay-time component in the derived impulse response function. This is because the population of the initially excited state is considered to be the excitation function. This spectral overlap component is easily quantified, and allows the emission spectra of the F and R states to be calculated. This deconvolution procedure requires one favorable circumstance, which is the ability to choose a wavelength at which only the initially excited state is emitting. We tested our procedure on the excited state protonation of acridine and the excited-state deprotonation of 2-naphthol. The former reaction is essentially irreversible, whereas depending upon pH the dissociation of 2-naphthol can be reversible. We demonstrated that this procedure, which we call differential-wavelength deconvolution, revealed the individual spectra and simplified determination of the kinetic constants from the time-resolved decays. Without differential-wavelength deconvolution considerably more complex methods are required. We expect this procedure to greatly facilitate the use of pulse fluorometry methods in the analysis of excited-state processes.

1. Introduction

The technique of fluorescence spectroscopy is widely used in biochemical research. One advantage of this method is high sensitivity, but perhaps a more important property is the natural time-window on the nanosecond time scale. Molecular events on this time scale affect the fluorescence spectroscopic observables and these rapid events can therefore be quantified. For example, the widely used measurements of fluorescence anisotropy are actually measurements of the average angular displacement of the fluorophore during the time between light absorption and subsequent emission. Increasingly, fluorescence measurements of time-dependent processes other than rotational diffusion are being used to examine the dynamic properties of biological macromolecules [1,2]. Examples of these excited-state reactions include excimer and exciplex formation in membranes [3,4], energy transfer between membrane- and/or protein-bound chromophores [5,6], ex-

0301-4622/82/0000-0000/$02.75

cited-state ionizations of biopolymer-bound fluorophores [7] and dipolar relaxation of proteins and membranes around the newly created dipole moments of the excited states [8–12]. Similar excited-state reactions have been used in investigations of the physical and dynamic properties of chemical polymers, as is summarized in a recent publication [13].

Many excited-state processes, with exceptions such as dipolar relaxation, can be accurately represented by a two-state model. Subsequent to excitation the fluorophore can react reversibly (or irreversibly) to form a new species with a distinct emission spectrum (fig. 1). The emission spectrum of the reacted state (R) is frequently shifted to longer wavelengths relative to that of the initially excited state (F). Generally, one wishes to determine the emission spectra of these individual species and the kinetic constants which determine their lifetimes and interconversion rates. Such determinations have been performed using steady-state measurements and the complementary techniques of pulse- and phase-modulation fluorometry [14–17].

In recent publications we described the theory and application of phase-modulation methods for the analysis of excited-state reactions [14,15]. One interesting conclusion was the realization that the kinetic constants of the reacted state could be directly determined from the phase or modulation differences between wavelength regions of the emission spectra characteristic of the F and R states. Upon further analysis we realized that similar procedures could be applied in pulse fluorometric methods. In this report we propose differential deconvolution of the time-resolved decays of fluorescence intensity at various wavelengths. To illustrate the advantages of this novel technique we first describe the nature of time-resolved decays of fluorescence for molecules which undergo excited-state reactions.

For a reversible two-state reaction the decay at all wavelengths is doubly exponential [16]. The measured decay times are independent of wavelength but the preexponential factors are wavelength dependent. Unfortunately, these four parameters each depend upon all the kinetic constants of the system. As a result, calculation of the physical quantities of interest, which are the individual emission spectra and the rate constants for emission and reaction, is complex. Differential-wavelength deconvolution is a simple method which eliminates this complexity and allows the direct experimental determination of the decay rates of the reacted state and the fractional fluorescence intensities of each state in the regions of spectral overlap. This procedure is conceptually simple. Assume that the emission on the blue side of a spectrum is due only to the unreacted state (fig. 2). The time-resolved intensity at this wavelength (λ_0) represents the population of the F

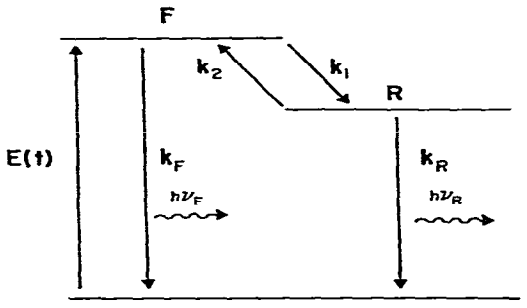

Fig. 1. Model for a reversible excited-state reaction.

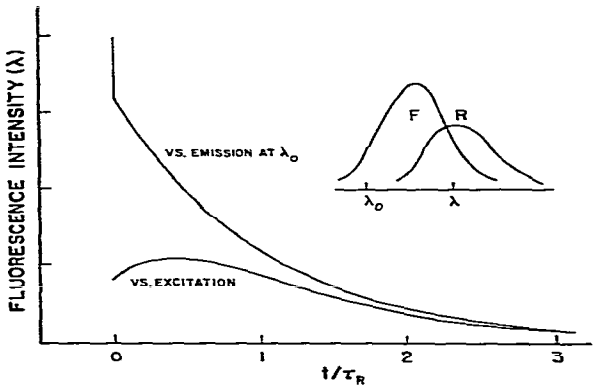

Fig. 2. Intuitive presentation of differential-wavelength deconvolution. The figure shows the impulse response of the fluorescence at λ obtained by deconvolution of this decay versus the excitation pulse and the emission decay at λ_0.

state. The F state is the source of excited molecules in the R state, just as the time profile of the exciting pulse describes the time-dependent excitation of the F state. It is known that deconvolution of the F state emission using the excitation light pulse reveals the decay constants of the F state. In this paper we demonstrate, both theoretically and experimentally, that deconvolution of the R state emission using the F state emission directly yields the decay times of the R state. This direct determination of kinetic constants of the R state is considerably simpler than analysis of the time-resolved fluorescence of the R state obtained relative to the exciting pulse. This procedure also simplifies the determination of the emission spectra of the F and R states. Frequently, these spectra overlap. Since the F state emission is used as the 'excitation function' any overlap of its emission with the R state at a longer wavelength (λ) appears to have the same time profile as the exciting pulse. Since our least-squares fit [18,19] uses a sum of exponentials, this term appears as a short-lived component with an apparent decay time near zero (fig. 2). The fractional amplitude of this component reveals the fractional intensity of the F state at wavelength λ where its emission overlaps with the R state.

We describe the use of differential-wavelength deconvolution in the analysis of two excited-state reactions. The first reaction examined was the excited-state protonation of acridine by ammonium ion. This reaction is essentially irreversible and has been studied in detail [15,17]. The second reaction we examined was the excited-state dissociation of 2-naphthol [16]. Depending upon the pH this reaction can be either reversible or irreversible. In both instances we used differential-wavelength deconvolution to calculate the individual emission spectra and the intrinsic decay rates of the reacted states. For the reversible dissociation of 2-naphthol we experimentally demonstrated that differential-wavelength deconvolution results in the simplification of the complex decay times to those representative of the reacted state. The procedure of differential-wavelength deconvolution is easy to implement using existing procedures and software and does not significantly increase the time required for data acquisition and analysis. Moreover, this procedure was useful for the study of solvent relaxation around a tryptophan derivative in a viscous solvent [20]. We expect differential-wavelength deconvolution to simplify the analysis of time-resolved decays involving excited-state reactions, increase the precision of the analysis, and thereby increase the usefulness of pulse fluorometric methods in the analysis of excited-state processes.

2. Theory

2.1. Time-resolved decays of fluorescence for reversible two-state reactions

The theory and usefulness of differential-wavelength deconvolution are most easily understood following a summary of the spectroscopic properties of fluorophores which undergo reactions and spectral shifts in the excited state. Hence, we describe reversible and irreversible two-state reactions. The excited molecule is assumed to exist in one of two states (fig. 1). Each state has a distinct emission spectrum and the kinetic constants of each state are independent of emission wavelength. This model appears to describe adequately processes such as excited-state protonation and deprotonation [16,17] and formation of excimers and exciplexes [21]. However, this model is not strictly applicable to solvent relaxation, which may be best described by continuous or multiple-step relaxation models [22,23].

In this model for a reversible two-state reaction the initially excited (F) and relaxed (R) states have different decay rates, k_F and k_R, which include the rates of radiative and nonradiative decay. The forward and reverse rate constants, k_1 and k_2, respectively, are written in this form for simplicity. For the excited-state protonation of acridine one would have $k_1 = k_1'[NH_4^+]$ and for the excited-state protonation of 2-naphtholate one has $k_2 = k_2'[H^-]$. The kinetic equations describing this system are

$$-\frac{d[F]}{dt} = (k_F + k_1)[F] - k_2[R] - E(t) \quad (1)$$

$$-\frac{d[R]}{dt} = (k_R + k_2)[R] - k_1[F] \quad (2)$$

where [F] and [R] are the populations of these states and $E(t)$ is the time profile of the excitation. Following return to the ground state this equilibrium is quickly reestablished and the extent of ground-state depopulation is small. Hence, we have not explicitly included the ground states in our kinetic equations or in fig. 1. The solution to these kinetic equations has been described previously with the boundary conditions $[F]=[F_0]$ and $[R]=0$ at $t=0$ [16,24]. The fluorescence decays of the F and R states following δ-pulse excitation are given by

$$I_F(\lambda,t)=\alpha_1(\lambda)e^{-t/\tau_1}+\alpha_2(\lambda)e^{-t/\tau_2} \tag{3}$$

$$I_R(\lambda,t)=\beta_1(\lambda)e^{-t/\tau_1}+\beta_2(\lambda)e^{-t/\tau_2} \tag{4}$$

Defining $\gamma_F=k_F+k_1$ and $\gamma_R=k_R+k_2$, the decay times are given by

$$\tau_1^{-1},\tau_2^{-1}=1/2\left\{(\gamma_F+\gamma_R)\mp\left[(\gamma_R-\gamma_F)^2+4k_1k_2\right]^{1/2}\right\} \tag{5}$$

and the preexponential factors are given by

$$\alpha_1(\lambda)=C_F(\lambda)[F_0]\frac{(\gamma_F-\gamma_2)\Gamma_F}{\gamma_1-\gamma_2} \tag{6}$$

$$\alpha_1(\lambda)=C_F(\lambda)[F_0]\frac{(\gamma_1-\gamma_F)\Gamma_F}{\gamma_1-\gamma_2} \tag{7}$$

$$-\beta_1(\lambda)=\beta_2(\lambda)=\frac{C_R(\lambda)k_1[F_0]\Gamma_F}{\gamma_1-\gamma_2} \tag{8}$$

In these equations $\gamma_1=\tau_1^{-1}$, $\gamma_2=\tau_2^{-1}$, Γ_F and Γ_R are the emission rates, and $C_F(\lambda)$ and $C_R(\lambda)$ the emission spectra of species F and R normalized to unit area:

$$C_F(\lambda)=\frac{f_F(\lambda)}{\int_0^\infty f_F(\lambda)d\lambda} \tag{9}$$

$$C_R(\lambda)=\frac{f_R(\lambda)}{\int_0^\infty f_R(\lambda)d\lambda} \tag{10}$$

where $f_F(\lambda)$ and $f_R(\lambda)$ are the numbers of quanta emitted at wavelength λ by F and R species, respectively. It is useful to note that for the R state the preexponential factors are equal in magnitude but have opposite signs.

At any given wavelength the time-resolved decay of fluorescence is given by

$$I(\lambda,t)=I_F(\lambda,t)+I_R(\lambda,t) \tag{11}$$

where the individual decays of F and R states are described by eqs. 3 and 4. Substitution of eqs. 3 and 4 into eq. 11 results in

$$I(\lambda,t)=\frac{[F_0]}{\gamma_1-\gamma_2}[C_F(\lambda)\Gamma_F(\gamma_F-\gamma_2)-C_R(\lambda)k_1\Gamma_R]e^{-t/\tau_1}+\frac{[F_0]}{\gamma_1-\gamma_2}[C_F(\lambda)\Gamma_F(\gamma_1-\gamma_F)+C_R(\lambda)k_1\Gamma_R]e^{-t/\tau_2} \tag{12}$$

Thus, at any given wavelength the decay of fluorescence is doubly exponential and the decay times are independent of the emission wavelength. The decay times are each dependent upon the four kinetic constants of the system. The preexponentials are complex factors which are dependent upon both the spectral distributions and the kinetic constants of both species.

Generally, we are interested in the absolute spectral intensities f_F and f_R, and we can replace the normalized intensities $C_F(\lambda)$ and $C_R(\lambda)$ with these values in the following manner. Consider the steady-state conditions and let $[F]_{ss}$ and $[R]_{ss}$ be the respective steady-state populations. Then

$$\frac{[R]_{ss}\Gamma_R}{[F]_{ss}\Gamma_F}=\frac{\int_0^\infty f_R(\lambda)d\lambda}{\int_0^\infty f_F(\lambda)d\lambda} \tag{13}$$

On the other hand eq. 2 results in

$$\frac{[R]_{ss}}{[F]_{ss}}=\frac{k_1}{\gamma_R} \tag{14}$$

Using eqs. 9, 10, 13 and 14 it is easy to obtain eq. 12 in the form

$$I(\lambda,t)=C\left[A_1(\lambda)e^{-t/\tau_1}+A_2(\lambda)e^{-t/\tau_2}\right] \tag{15}$$

where

$$C=\frac{[F_0]k_1\Gamma_R}{(\gamma_1-\gamma_2)\int_0^\infty f_R(\lambda)d\lambda} \tag{16}$$

$$A_1(\lambda)=f_F(\lambda)\frac{\gamma_F-\gamma_2}{\gamma_R}-f_R(\lambda) \tag{17}$$

$$A_2(\lambda)=f_F(\lambda)\frac{\gamma_1-\gamma_F}{\gamma_R}+f_R(\lambda) \tag{18}$$

2.2. Resolution of spectra from time- and wavelength-resolved decays of fluorescence

The experimentally obtained decay of $I(\lambda,t)$ described by eq. 15 (two decay times τ_1 and τ_2 and

the ratio A_2/A_1) allows one to resolve the individual spectra and simultaneously find γ_F and γ_R. This requires, however, the existence of a spectral region where only the F species emits, which fortunately is a common occurrence. Let γ_0 be within this spectral range. The value of γ_F can be obtained in the following manner. Consider the decay $I(\lambda_0,t)$ (eq. 12). Since $C_R(\lambda_0)=0$ then

$$I(\lambda_0,t)=\frac{[F_0]\Gamma_F}{\gamma_1-\gamma_2}C_F(\lambda_0)\left[a_1e^{-t/\tau_1}+a_2e^{-t/\tau_2}\right] \tag{19}$$

where $a_1=\gamma_F-\gamma_2$ and $a_2=\gamma_1-\gamma_F$. Therefore, γ_F can be calculated as:

$$\gamma_F=\frac{a_1\gamma_1+a_2\gamma_2}{a_1+a_2} \tag{20}$$

From eq. 5 for γ_1 and γ_2 one can find

$$\gamma_1+\gamma_2=\gamma_F+\gamma_R \tag{21}$$

Thus, the value of γ_R can also be determined. Finally, the ratio of the preexponential factors in eq. 15 can be used to resolve the spectra of the F and R species:

$$\frac{f_F}{f_R}=\gamma_R\frac{A_1+A_2}{A_1(\gamma_2-\gamma_R)+A_2(\gamma_1-\gamma_R)} \tag{22}$$

For simplicity we write f_F and f_R instead of $f_F(\lambda)$ and $f_R(\lambda)$.

Of course the calculation of the fractional intensities is now trivial:

$$\frac{f_F}{f_F+f_R}=\gamma_R\frac{A_1+A_2}{A_1\gamma_2+A_2\gamma_1} \tag{23}$$

$$\frac{f_R}{f_F+f_R}=\frac{A_1(\gamma_2-\gamma_R)+A_2(\gamma_1-\gamma_R)}{A_1\gamma_2+A_2\gamma_1} \tag{23}$$

The spectra of the individual species may be calculated from the fractional intensities and the steady-state emission spectrum $I(\lambda)$.

$$I_F(\lambda)=\frac{f_F}{f_F+f_R}I(\lambda) \tag{24}$$

$$I_R(\lambda)=\frac{f_R}{f_F+f_R}I(\lambda) \tag{24}$$

Eqs. 23 and 24 can be used to resolve the individual spectra at wavelengths where the decay is doubly exponential. However, at some wavelength where these spectra overlap the decay of $I(\lambda,t)$ is practically a single exponential ($A_2=0$), and the experimentally fitted values of τ_2 are meaningless. However, since τ_1 and τ_2 are independent of wavelength, these values, measured at other wavelengths, can be used to calculate the fractional intensities.

$$\frac{f_F}{f_F+f_R}=\frac{\gamma_R}{\gamma_2} \tag{25}$$

$$\frac{f_R}{f_F+f_R}=1-\frac{\gamma_R}{\gamma_2} \tag{26}$$

This procedure requires calculation of γ_F from eq. 20 and γ_R from eq. 21.

When the excited-state reaction is irreversible, $k_2=0$ and eq. 5 yields

$$\gamma_1=\gamma_R,\ \gamma_2=\gamma_F. \tag{27}$$

This means that the decay rates of the F and R species can be measured directly. Eqs. 23 and 24 simplify to:

$$\frac{f_F}{f_F+f_R}=\gamma_1\frac{A_1+A_2}{A_1\gamma_2+A_2\gamma_2}$$

$$\frac{f_R}{f_F+f_R}=A_1\frac{\gamma_2-\gamma_1}{A_1\gamma_2+A_2\gamma_2} \tag{28}$$

We note that the expressions for the fractional intensities of the individual components (eqs. 23 and 24) are considerably more complex than those required to resolve the spectra of two directly excited fluorophores, i.e., a heterogeneous mixture of fluorophores. If the subscripts A and B refer to these individual fluorophores, then

$$\frac{f_A}{f_A+f_B}=\frac{\alpha_A\tau_A}{\alpha_A\tau_A+\alpha_B\tau_B}$$

$$\frac{f_B}{f_A+f_B}=\frac{\alpha_B\tau_B}{\alpha_A\tau_A+\alpha_B\tau_B}. \tag{29}$$

where α_A and α_B are the preexponential factors and τ_A and τ_B are the respective decay times. These simpler expressions are comparable to those used for spectral resolution following differential-wavelength deconvolution (eq. 55). However, the latter equations allow spectral resolution of species involved in an excited-state reaction whereas the former (eq. 29) apply only to ground-state heterogeneity.

2.3. Resolution of states using differential-wavelength deconvolution

We now describe a new competitive method of resolving the component spectra and finding the

decay rates in the case of reversible reactions ($k_2 \neq 0$). For these purposes we introduce the concept of internal convolution and the experimental method of differential wavelength deconvolution. Eq. 2 may be rewritten in the form

$$\frac{d[R](t)}{dt} + \gamma_R[R](t) = k_1[F](t). \quad (30)$$

Using the variation of parameters method, the solution may be written as

$$[R](t) = P(t)D(t) \quad (31)$$

where $D(t)$ is the solution to the homogeneous equation

$$\frac{dD(t)}{dt} + \gamma_R D(t) = 0 \quad (32)$$

Of course then

$$D(t) = a\,e^{-\gamma_R t} \quad (33)$$

with a being an arbitrary constant. It is convenient to use $a = k_1$. Substitution of eqs. 31–33 into eq. 30 yields

$$\frac{dP(t)}{dt} = [F](t)e^{\gamma_R t} \quad (34)$$

integration of this equation with a boundary condition $P(0) = 0$ leads to:

$$P(t) = \int_0^t [F](t')e^{\gamma_R t'}dt' \quad (35)$$

Finally, combining eqs. 31 and 35, one obtains

$$[R](t) = k_1 \int_0^t [F](t')e^{-\gamma_R(t-t')}dt' \quad (36)$$

This is an important result which means that the decay of the R species following δ-pulse excitation is an internal convolution of the decay of the F species and the intrinsic decay of the R species (the one that would be observed if it could be excited directly). Eq. 36 is valid irrespective of the value of k_2 or, in other words, both for the irreversible and reversible reactions. It should be stressed that eq. 36 is a direct consequence of eq. 2 and no additional assumptions are necessary to derive it. It can be shown that instead of [R] and [F] we can use the experimentally obtained decays $[R]_c$ and $[F]_c$ for any arbitrary excitation function $E(t)$. This function can include the lamp pulse and the response of the detecting system. Eq. 36 will still be valid not only for

$$[R](t) = [F](t) \otimes D(t) \quad (37)$$

but also for

$$[R]_c(t) = [F]_c(t) \otimes D(t) \quad (38)$$

where ⊗ denotes the convolution integral and $D(t) = k_1 e^{-\gamma_R t}$ is the intrinsic decay of the R species. For an arbitrary excitation function $E(t)$

$$[R]_c(t) = E(t) \otimes [R](t) \quad (39)$$

$$[F]_c(t) = E(t) \otimes [F](t) \quad (40)$$

The proof of eq. 38 is as follows. Since convolution is associative, eqs. 37 and 39 yield

$$[R]_c(t) = E(t) \otimes [[F](t) \otimes D(t)] = [E(t) \otimes [F](t)] \otimes D(t) \quad (41)$$

Substitution of eq. 40 into eq. 41 results in

$$[R]_c(t) = [F_c](t) \otimes D(t)$$

which is eq. 38. Thus, the decay of the R species is an internal convolution of the decay of the F species and the intrinsic decay of the R species, irrespective of the time dependence of the excitation function. Harmonic excitation (phase and modulation fluorometry) can also be included [14,15].

The important consequence of the above considerations is that the deconvolution of the experimental decay of the intensity of the R species with the experimental decay of the intensity of the F species as an excitation function gives the intrinsic single-exponential decay law of the R species and thus γ_R. To perform this deconvolution one needs to find a spectral region where only the F species emits and to use the decay of this emission as the excitation function. This procedure will be called the differential-wavelength deconvolution. An interesting and useful feature of this procedure is its ability to easily resolve the spectra of the two species even for the reversible reactions. To demonstrate this let us recall eq. 11.

$$I(\lambda,t) = I_F(\lambda,t) + I_R(\lambda,t)$$

The individual intensities I_F and I_R can be written as

$$I_F(\lambda,t) = C_F(\lambda)\Gamma_F[F](t) \quad (42)$$

$$I_R(\lambda,t)=C_R(\lambda)\Gamma_R[R](t) \quad (43)$$

where $C_F(\lambda)$ and $C_R(\lambda)$ are normalized emission spectra defined by eqs. 9 and 10. Let us introduce the observed intensities I_{Fc} and I_{Rc} defined as

$$I_{Fc}(\lambda,t)=E(t)\otimes I_F(\lambda,t)=C_F(\lambda)\Gamma_F\{E(t)\otimes[F](t)\}$$
$$=C_F(\lambda)\Gamma_F[F]_c(t) \quad (44)$$

$$I_{Rc}(\lambda,t)=E(t)\otimes I_R(\lambda,t)=C_R(\lambda)\Gamma_R\{E(t)\otimes[R](t)\}$$
$$=C_R(\lambda)\Gamma_R[R]_c(t) \quad (45)$$

Thus, the total observed intensity I_c is equal to

$$I_c(\lambda,t)=C_F(\lambda)\Gamma_F[F]_c(t)+C_R(\lambda)\Gamma_R[R]_c(t) \quad (46)$$

Combining eqs. 9, 10, 13, 14 and 46, we obtain

$$I_c(\lambda,t)=C'\{f_F(\lambda)k_1[F]_c(t)+f_R(\lambda)\gamma_R[R]_c(t)\} \quad (47)$$

where

$$C'=\frac{\Gamma_R}{\gamma_R\int_0^\infty f_R(\lambda)d\lambda}.$$

Recalling that the convolution of any function with the δ-function results in the same function,

$$[F]_c(t)=[F]_c(t)\otimes\delta(t), \quad (48)$$

that the R species does not contribute to the emission at λ_0, and eq. 38, the total observed decay can be written as

$$I_c(\lambda,t)=C''(\lambda_0)I_{Fc}(\lambda_0,t)\otimes[f_F(\lambda)k_1\delta(t)+f_R(\lambda)\gamma_R D(t)] \quad (49)$$

where $C''(\lambda_0)=C'/C_F(\lambda_0)\Gamma_F$ (see eq. 46) and λ_0 is the wavelength at which the F state can be observed exclusively. The differential-wavelength deconvolution should yield the expression

$$f_F(\lambda)k_1\delta(t)+f_R(\lambda)\gamma_R D(t)$$

However, the deconvolution algorithms usually assume only exponential time dependences. The δ-function is then approximated by an exponential decay $G(t)=a_0e^{-t/\tau_0}$ with $\tau_0\to 0$, $a_0\tau_0=1$. This can be understood by noting that the condition which must be fulfilled by the δ-function

$$\int_0^\infty\delta(t)dt=1 \quad (50)$$

is also fulfilled by $G(t)$, since

$$\lim_{\tau_0\to 0}\int_0^\infty a_0e^{-t/\tau_0}dt=a_0\tau_0=1 \quad (51)$$

Thus, eq. 49 can be written as:

$$I_c(\lambda,t)=C''(\lambda_0)I_{Fc}(\lambda_0,t)$$
$$\otimes\left[f_F(\lambda)k_1a_0e^{-t/\tau_0}+f_R(\lambda)k_1\gamma_Re^{-t/\tau_R}\right] \quad (52)$$

where $\tau_R=\gamma_R^{-1}$, or

$$I_c(\lambda,t)=k_1C''(\lambda_0)I_{Fc}(\lambda_0,t)$$
$$\otimes\left[\alpha_0(\lambda)e^{-t/\tau_0}+\alpha_R(\lambda)e^{-t/\tau_R}\right] \quad (53)$$

where $\alpha_0(\lambda)=f_F(\lambda)a_0$ and $\alpha_R(\lambda)=f_R(\lambda)\gamma_R=f_R(\lambda)/\tau_R$.

Differential-wavelength deconvolution will therefore yield a double-exponential decay with one of the decay times (τ_0) close to zero and the other being the intrinsic decay time of the R species. Furthermore, recalling $a_0\tau_0=1$, the products $\alpha_0\tau_0$ and $\alpha_R\tau_R$ are simply equal to:

$$\alpha_0(\lambda)\tau_0=f_F(\lambda)$$
$$\alpha_R(\lambda)\tau_R=f_R(\lambda) \quad (54)$$

and thus, the individual spectra of F and R species are easily obtained in this way. Alternatively, one may calculate the fractional intensities using equations similar to those used for the analysis of heterogeneous fluorescence.

$$\frac{f_F}{f_F+f_R}=\frac{\alpha_0\tau_0}{\alpha_0\tau_0+\alpha_R\tau_R}=\frac{I_F(\lambda)}{I(\lambda)}$$

$$\frac{f_R}{f_F+f_R}=\frac{\alpha_R\tau_R}{\alpha_0\tau_0+\alpha_R\tau_R}=\frac{I_R(\lambda)}{I(\lambda)} \quad (55)$$

These expressions are considerably simpler than those necessary when the deconvolution is performed versus the lamp pulse (eqs. 23 and 24). In addition, this method is free of the uncertainties at that wavelength where the decay of total fluorescence is single exponential (see eqs. 25 and 26). An important advantage of the differential-wavelength deconvolution method is also its ability to directly determine the intrinsic decay rate of the R species γ_R. γ_F can in turn be determined from eq. 21.

2.4. Multiple-step processes

The concept of internal convolution can also be applied to a multiple-step irreversible relaxation (or reaction) model [20]. If N_q represents the number of excited fluorophores in the q-th state, the

following system of equations is valid:

$$\frac{dN_n}{dt} = E(t) - (nk + \gamma)N_n$$
$$\frac{dN_q}{dt} = (q+1)kN_{q+1} - (qk + \gamma)N_q$$
$$\frac{dN_0}{dt} = kN_1 - \gamma N_0. \quad (56)$$

Here $E(t)$ is the excitation intensity time profile, qk the rate of the relaxation of the q-th state, k a constant, $q = 0, \ldots, n$, and γ the decay rate in the absence of relaxation. N_n and N_0 are the populations of the initial and final states, respectively. In the limit of large n this model becomes equivalent to the continuous relaxation model of Bakhshiev et al. [22,23]. Obviously

$$\frac{dN_q}{dt} + (qk + \gamma)N_q = (q+1)kN_{q+1} \quad (57)$$

This is analogous to eq. 30 and as a consequence of that we obtain

$$N_q(t) = (q+1)k\int_0^t N_{q+1}(t')e^{-(qk+\gamma)(t-t')}dt' \quad (58)$$

Thus, the observed decay of the population of the q-th state is a convolution of the population of the $(q+1)$-th state and the intrinsic decay of the q-th state. This is true irrespective of the number of exponential components characterizing the decay of the given state which is $n - q + 1$. The practical application of the above consideration may be hindered, however, because of the substantial spectral overlap of the consecutive states. Iterative application of eq. 58 leads to the following relationship:

$$N_q(t) = \frac{n!}{q!}k^{n-q}N_q'(t) \otimes N_{q+1}'(t) \otimes \ldots \otimes N_n(t) \quad (59)$$

with N_q' describing the intrinsic decay of the q-th state

$$N_q'(t) = e^{-(qk+\gamma)t} \quad (60)$$

Thus, the decay of population of the q-th state is a convolution of the decay of the initial state n and the intrinsic decays of populations of all the consecutive states preceding and including state q.

2.5. Explicit equations for a three-state irreversible process

The concept of internal convolution can be used to reduce the number of exponentials to be analyzed in multiple-exponential decays. Consider, for instance, a three-state case. The decay of the final-state population is described by:

$$N_0(t) = N_{2,0}[e^{-(2k+\gamma)t} - 2e^{-(k+\gamma)t} + e^{-\gamma t}] \quad (61)$$

where $N_{2,0}$ is the population of the initial state at $t = 0$. Using eq. 59 for $q = 0$, $n = 2$, which is

$$N_0(t) = 2k^2N_0'(t) \otimes N_1'(t) \otimes N_2(t) \quad (62)$$

one obtains the explicit formula

$$N_0(t) = 2k\int_0^t N_2(t')[e^{-\gamma(t-t')} - e^{-(k+\gamma)(t-t')}]dt'. \quad (63)$$

Thus, the decay of the final-state population is the internal convolution of the decay of the initial-state population $N_2(t)$ and the double-exponential decay which would be observed if the intermediate state could be excited directly. Of course the following relations also hold:

$$N_1(t) = 2k\int_0^t N_2(t')e^{-(k+\gamma)(t-t')}dt' \quad (64)$$

$$N_0(t) = k\int_0^t N_1(t')e^{-\gamma(t-t')}dt' \quad (65)$$

The experimental advantage of eq. 63 is the ability to simplify the complex kinetics of a two-step (three-state) reaction to the comparably simple kinetics of a one-step reaction. Following deconvolution versus the initially excited state, one can examine the derived impulse response functions using the more familiar concepts applicable to a one-step reaction. More specifically, if following deconvolution versus the initially excited state a term with a negative preexponential factor is still observed on the long-wavelength side of the emission, one may confidently infer the existence of an intermediate species. If this intermediate state could be selectively observed by optical filtering then the intrinsic emission rate of this final state could be obtained from deconvolution versus the emission from the intermediate state. Unfortunately, in the case of fluorescence, spectral overlap of states will generally prevent the application

of this further simplification. This limitation may be less restrictive in the application of these concepts using other methods of instrumental analysis.

2.6. Reversible multiple-step processes

In the case of the reversible multiple-step relaxation process with the reverse rate $k_2(q \rightarrow q+1)$, eq. 56 are no longer valid. Eq. 57 then becomes

$$\frac{dN_q(t)}{dt} + (qk_1 + \gamma)N_q(t) = (q+1)k_1 N_{q-1}(t) - k_2 N_{q-1}(t) \tag{66}$$

This is equivalent to the following convolution formula:

$$N_q(t) = [(q+1)k_1 N_{q+1}(t) - k_2 N_{q-1}(t)] \otimes N'_q(t) \tag{67}$$

for $q = 1, \ldots n-1$.

Eq. 67 means that the decay of population of the q-th state is a convolution of its intrinsic decay with the decays of the neighboring states $q-1$, $q+1$, since both of them are the source of the q-th state population. In this case, differential-wavelength deconvolution does not seem to help in the analysis of pulse data, except for the initial and final states where only one adjacent state serves as the source. However, in instances where analytical procedures can quantify the concentrations of the adjacent states, the principle of internal convolution may assist in the analysis of even reversible multiple-step reactions.

3. Materials and methods

Time-resolved decays of fluorescence were measured with a single-photon pulse fluorometer from Photochemical Research Associates. Deconvolution of these time-resolved decays was performed using the method of least squares [18,19]. For each emission wavelength where decay times were needed we measured the time profiles of the excitation pulse, the emission of the unreacted species (F) and the emission at the longer wavelength of interest. The data for the longer wavelength were deconvolved using either the lamp profile or the F state response. The F state responses were measured at 350 and 400 nm for 2-naphthol and acridine, respectively. For pulse measurements the following conditions were used for 2-naphthol and acridine, respectively: excitation wavelength, 330 and 348 nm; excitation band pass, 8 and 16 nm, emission band pass, 8 and 8 nm; temperature, 24 and 20°C; fluorophore concentration, 5×10^{-5} and 2×10^{-5} M. The samples were not purged with inert gas. Steady-state fluorescence spectra were collected under similar conditions except the excitation band passes were 2 and 8 nm. In addition, the emission spectra of acridine were collected through polarizers set at the magic-angle positions. All other measurements were performed

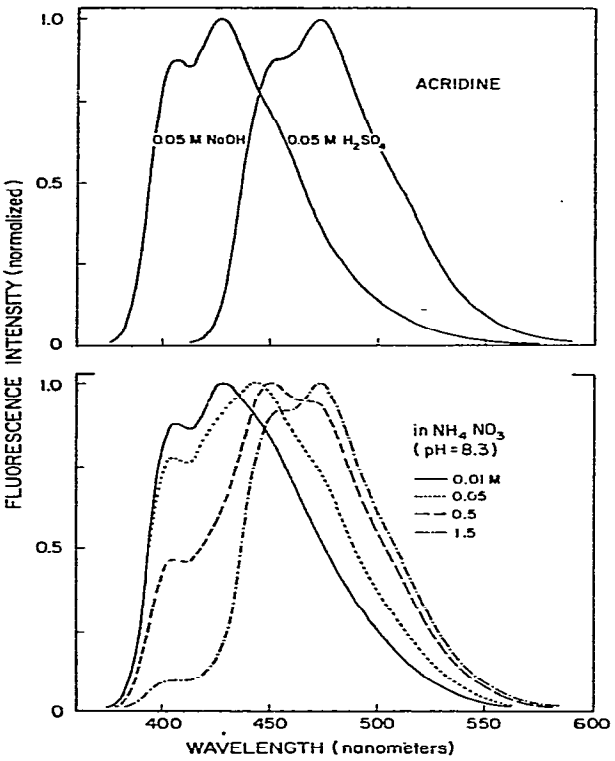

Fig. 3. Steady-state emission spectra of acridine. Spectra are shown for acridine in 0.05 M NaOH and in 0.05 M H_2SO_4 (top panel). The lower panel shows spectra in various concentrations of ammonium nitrate: pH 8.3, 20°C.

Table 1
Decay times for acridine fluorescence

Solvent	Emission wavelength (nm)	τ (ns)	χ^2
0.05 M NaOH	400	10.5	1.02
	560	10.1	1.27
0.1 M H_2SO_4	560	30.8	1.13

without polarizers. Insofar as possible, solution conditions were identical to those described previously [16,17].

4. Results

4.1. Excited-state protonation of acridine

For our initial experimental tests of differential-wavelength deconvolution we chose to examine the excited-state protonation of acridine by ammonium ions. This reaction has been studied in detail by both pulse- and phase-modulation methods [15,17] and is essentially irreversible under our experimental conditions. Fig. 3 shows the steady-state emission spectra of acridine in basic and acidic solution. At high pH the emission results exclusively from neutral acridine, and in acidic solution the emission is red shifted and characteristic of the acridinium cation. Increasing concentrations of ammonium, which serves as a proton donor, progressively quench the emission from neutral acridine. Simultaneously, one observes increasing emission from the acridinium cation. Examination of these spectra reveals a wavelength region from 380 to 410 nm where emission results from only the F state, neutral acridine. Hence, the nonoverlap condition for differential-wavelength deconvolution is satisfied. At wavelengths longer than 450 nm the emission is dominated by that resulting from acridinium, but significant contributions from both acridine and acridinium are present at all these longer wavelengths. We chose 400 nm to select for emission from acridine and 560 nm to select, to the extent possible, for emission from acridinium.

For each of the individual species the lifetimes are expected to be single exponentials irrespective of emission wavelength. Data for acridine in acidic and basic solution which confirm this prediction are listed in table 1. In 0.1 M H_2SO_4 the decay time was 30.8 ns at 560 nm, in excellent agreement with that measured previously [17], and this same

Table 2
Decay time for acridine fluorescence in ammonium nitrate

$[NH_4NO_3]$ (M)	Emission wavelength (nm)	Deconvolution versus lamp pulse				Deconvolution of 560 nm vs. 400 nm response			
		τ_1 (ns)	τ_2 (ns)	$\alpha_1\tau_1$ (%)	χ^2	τ_0 (ns)	τ_R (ns)	$\alpha_0\tau_0$ (%)	χ^2
0.1	400	5.5	–	98.7	1.20				
	560	⟨5.4⟩ [a]	30.8	8.3	1.21	0.06	31.0	9.6	1.20
0.5	400	2.0	–		1.42				
	560	⟨1.9⟩	27.7		1.06	0.01	27.7		1.07
1.0	400	1.2	–	97.7	5.29				
	560	⟨0.9⟩	24.7	3.4	1.52	0.05	24.4	1.4	1.17
1.5	400	0.8	–	95.8	2.34				
	560	⟨0.65⟩	23.0	2.4	–	0.31	22.3	1.2	1.0
2.0	400	0.40	–	95.8	2.66				
	560	⟨1.08⟩	21.1	–	0.96	0.01	20.2	0.7	1.12

[a] The brackets ⟨⟩ indicate that this decay constant had a negative preexponential factor.

lifetime was observed at shorter emission wavelengths. No emission from acridinium was detectable at 400 nm, confirming the choice of this wavelength for selection of emission from the F state. In 0.05 M NaOH neutral acridine emission was detectable at both 400 and 560 nm, and the lifetime was 10.3 ± 0.2 ns, irrespective of wavelength.

More complex kinetic behavior was seen in acridine solutions which contained ammonium nitrate (table 2). At 400 nm the fluorescence decay was well represented by a single decay rate. As expected, the lifetime decreased with increasing concentrations of ammonium ion due to increased rates of protonation of excited acridine. For the irreversible reaction it is appropriate to equate decay rates with the lifetimes of the individual species (eq. 27) and the short lifetime is assigned to neutral acridine. At 560 nm the time-resolved intensities could be fitted using the doubly exponential model. The preexponential factor of the shorter decay time was negative, an observation which indicates that an excited-state process, rather than direct excitation, is at least partially responsible for the emission at longer wavelengths.

At all concentrations of ammonium ion a second longer-lived component is observed at 560 nm, and this component is due to the emission from acridinium. This decay time decreases at increased concentrations of ammonium nitrate due to quenching of acridinium fluorescence by this salt. If choice of 560 nm resulted in only the observation of acridinium fluorescence, it is known that the preexponential factors would be equal and opposite in sign [16]. The negative preexponential factor was, however, smaller than the positive one which indicates spectral overlap of acridine emission at 560 nm. As the ammonium concentration is increased this difference decreases, confirming its origin from neutral acridine.

4.2. Differential-wavelength deconvolution applied to acridine-acridinium

The excited-state protonation of acridine provides a simple test case for the method of differential-wavelength deconvolution. Since the reaction is irreversible under our conditions, the measured decay times can be equated with the lifetimes of the individual species. One can readily predict the outcome of deconvolving the response measured at 560 nm with that measured at 400 nm. Since the excited acridine (400 nm) is the source of acridinium fluorescence (560 nm) we expect the deconvolution procedure to yield a dominant component with the acridinium lifetime. Examination of table 2 shows that this is the case. The 20–30 ns component is retained following differential-wavelength deconvolution. In contrast, the shorter 1–5 ns components due to neutral acridine are no longer evident. After deconvolution versus the 400 nm response these shorter components are found as short-lived components (0.01–0.3 ns). These times are comparable to the resolution of our instrument. The origin of these 'zero-decay' time components is overlap of the emission from acridine and acridinium of 560 nm (eq. 53). If there were no spectral overlap at acridine fluorescence at 560 nm the measured decay would appear to be a single exponential. These initial results confirmed our prediction that we could measure the intrinsic lifetime of the R state and the extent of spectral overlap by differential-wavelength deconvolution.

To test the spectral resolving power of the differential-wavelength deconvolution we measured the fluorescence decays of acridine in 0.2 M ammonium nitrate at various emission wavelengths (fig. 4). As expected for a two-state reaction the apparent decay times were independent of emission wavelength. Of course, the preexponential factors were strongly dependent upon wavelength (data not shown). At wavelengths longer than 410 nm the 3.9 ns component has a negative preexponential factor. Upon deconvolution of these data versus the response at 400 nm the longer-lived component is retained, but the shorter component is replaced by a short-lived component ($\simeq 0.02$ ns). The fractional intensity of this component is near 100% at the shorter wavelengths, and decreases to about 6% at 560 nm. The appearance of the observed decays is seen in fig. 5, where we show the measured responses at various wavelengths. At short wavelengths (410 nm) the measured decay closely follows the decay of the 400 nm response. As the observation wavelength is increased, the fractional contribution of the

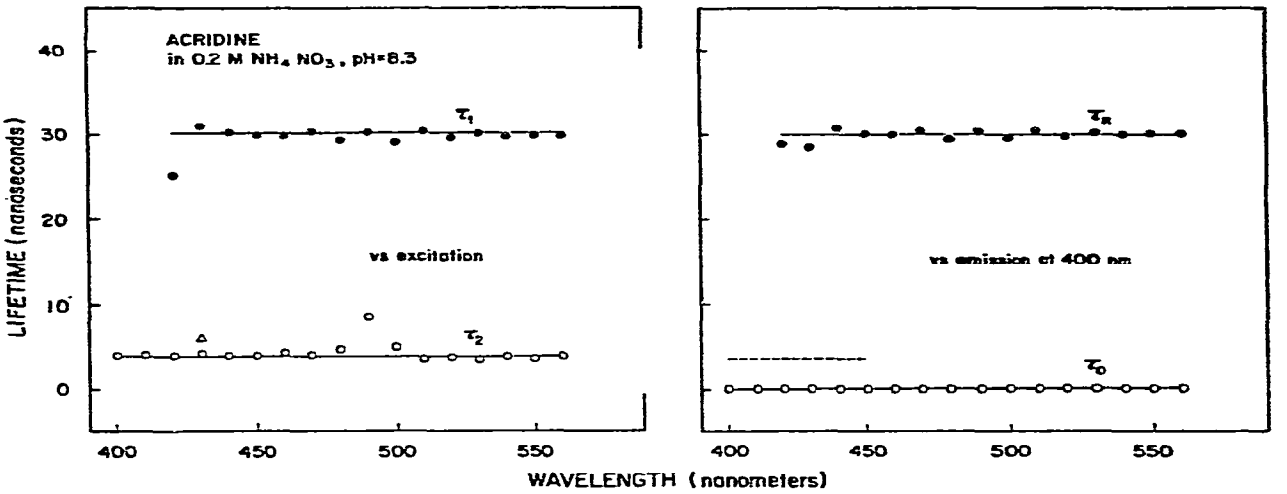

Fig. 4. Wavelength-dependent decay times for acridine on 0.2 M ammonium nitrate. Decay times are shown for deconvolution versus the lamp pulse and versus the emission at 400 nm.

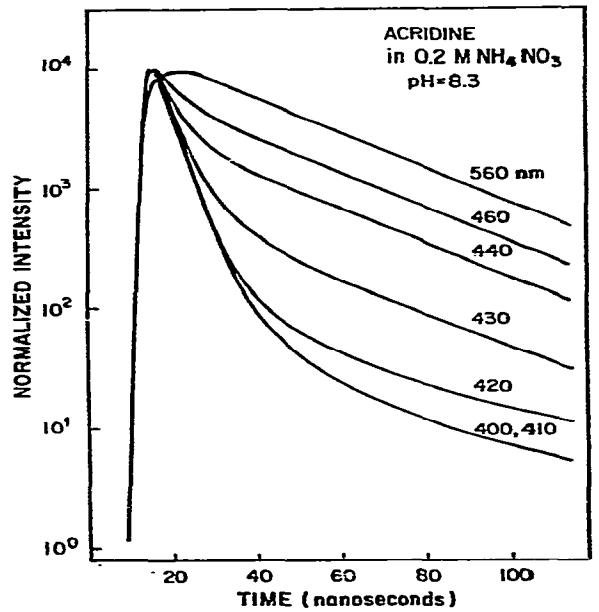

Fig. 5. Time-resolved decays of acridine at different emission wavelengths. Time-resolved decays are for acridine in 0.2 M NH_4NO_3, pH 8.3.

shorter-lived component decreases. At 560 nm the intensity of the short-lived component is small and not readily seen by visual examination.

We used the wavelength dependence of the $\alpha\tau$ products ($\alpha_0\tau_0$ and $\alpha_R\tau_R$) for the short-lived component to calculate the individual emission spectra

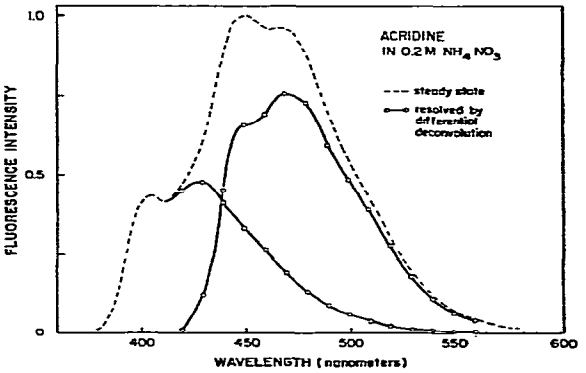

Fig. 6. Spectral resolution of the fluorescence from acridine and acridinium as obtained by differential-wavelength deconvolution.

of acridine and acridinium (fig. 6). The calculated spectra overlap precisely with the steady-state spectra obtained in basic and acidic solution, respectively. As described in section 2 such spectral resolution may be obtained without differential-wavelength deconvolution, but the required manipulations are more complex. Although the reproducibility of the individual values of α_0 and τ_0 is very poor, their product $\alpha_0\tau_0$ can be measured with high accuracy, resulting in excellent spectral resolution.

4.3. Excited-state dissociation of 2-naphthol

We chose the excited-state dissociation of 2-naphthol as a second example of the application of differential-wavelength deconvolution. At low pH the emission results from naphthol with an emission maximum at 357 nm (fig. 7). At high pH emission results primarily from the naphtholate anion, and is centered at 409 nm. At intermediate pH values emission from both species is observed. Examination of these spectra shows that at $\lambda \leq 350$ nm the naphthol-naphtholate system displays the nonoverlap condition necessary for differential-wavelength deconvolution. The advantage of this reaction is that it can be either reversible or irreversible, depending upon pH. At pH values near 3 the reaction is reversible, but at pH values above 6 the reaction is irreversible [16]. Hence, for the more complex reversible reaction, we can test

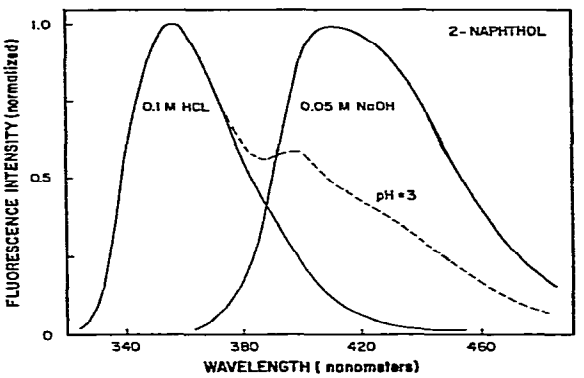

Fig. 7. Steady-state emission spectra of 2-naphthol. Spectra are shown in 0.1 M HCl, 0.05 M NaOH and in water at pH 3.0 (- - -), 24°C.

whether the simplified interpretation of the decay times and fractional intensities predicted by the theory of differential-wavelength deconvolution occurs in practice.

We measured the time-resolved decays of fluorescence at various wavelengths across the emission spectra (fig. 8). At pH 6.6 we obtained data characteristic of an irreversible reaction. On the blue side of the emission, where only naphthol emits, the decay was monoexponential. At longer wavelengths where both species emit the decay became doubly exponential. The fractional intensity of the 8.9 ns component increased with emission wavelength and at wavelengths greater than 390 nm this component had a negative preexponential factor (data not shown).

We also analyzed these time-resolved decays by differential-wavelength deconvolution (fig. 8). Again, two decay times were necessary to fit the decay. One of these was still 9.0 ± 0.1 ns, and is attributed to the intrinsic decay of naphtholate (τ_R). The second appeared as a short-lived component (0.3 ns) and is attributed to the naphthol emission at the longer wavelengths. The fractional intensities of these components allow calculation of the spectra of each species, as described by eqs. 54 and 55. These calculated spectra are not shown, but they overlap precisely with the steady-state spectra of naphthol and naphtholate.

A critical test of our procedure was provided by the reversible dissociation at pH 3. In this case the individual decay times, when deconvolved versus the lamp pulse, are complex functions of all the rate constants of the system (eq. 5). In contrast, deconvolution versus the 350 nm response should significantly simplify the interpretation of the two decay times so that one represents spectral overlap and the other is given by $\tau_2^{-1} = k_R + k_2'[H^+]$. Hence, we expect the two wavelength-independent decay times obtained by the usual deconvolution procedure to be replaced by two different decay times. Examination of fig. 8 shows that this is indeed the case. The decay times of 4.1 and 8.3 ns were replaced by 0.2 and 7.2 ns. The last value is characteristic of the intrinsic decay of naphtholate at pH 3 [16]. We conclude that the new deconvolution procedure does indeed simplify the analysis of the kinetic constants.

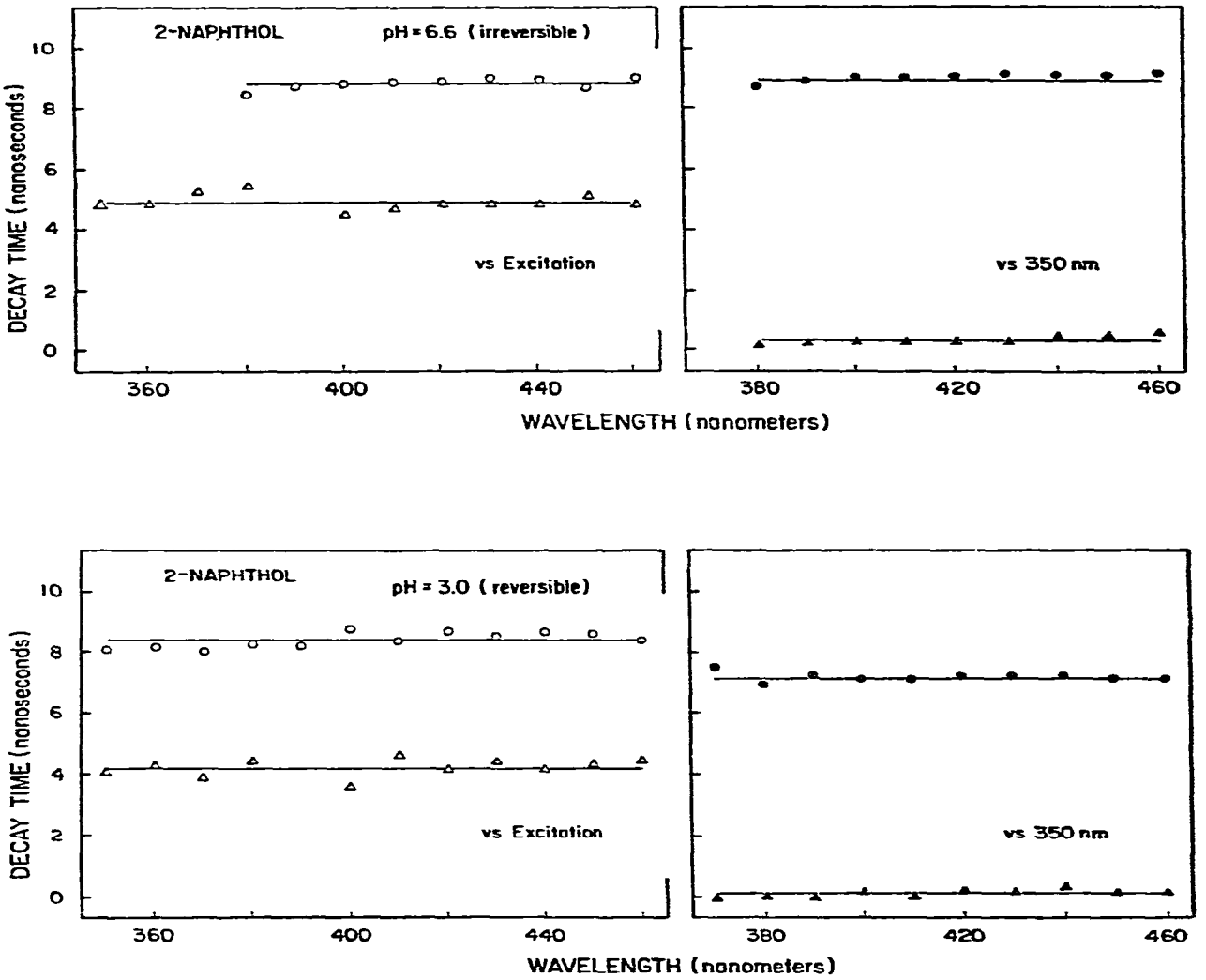

Fig. 8. Wavelength-dependent decay time of 2-naphthol. Decay times are shown for deconvolution versus the lamp pulse and versus the emission at 350 nm.

The simplification of the interpretation of the fractional intensities ($\alpha_i\tau_i$) provided by differential-wavelength deconvolution is illustrated in fig. 9. In this figure we show these values for deconvolution versus the lamp pulse and versus the 350 nm response. Interpretation of the values obtained from differential deconvolution is straightforward, this being the fractional intensity of either the F or R state. At 360 nm $\alpha_0\tau_0$ is unity since naphtholate does not emit at this wavelength (fig. 7). As the wavelength is increased $\alpha_0\tau_0$ decreases monotonically to about 0.07 at 460 nm,

indicating that the naphtholate emission is dominant at this longer wavelength. Of course, $\alpha_R\tau_R$ increases with wavelength in a complementary fashion.

Interpretation of the $\alpha_i\tau_i$ values obtained by deconvolution versus the lamp pulse is more complex. For example, at 360 nm, the values of both $|\alpha_1\tau_1|$ and $|\alpha_2\tau_2|$ are near 0.5 even though the emission is due to only naphthol. Interpretation of these values in terms of spectral intensities requires the use of eqs. 23 and 24. In addition, the individual values of $\alpha_i\tau_i$ become undetermined near 390 nm where the decay is almost a single exponential. At this wavelength alternative calculations are needed (eqs. 25 and 26). The new deconvolution procedure also eliminates this difficulty.

We used the fractional intensities ($\alpha_0\tau_0$ and $\alpha_R\tau_R$) in fig. 9 to calculate the spectra of naphthol and naphtholate (fig. 10). The spectral distributions of these individual spectra overlap precisely with the steady-state spectra of naphthol and naphtholate (fig. 7). Such precise overlap cannot be obtained using time-resolved emission spectra when the individual lifetimes are comparable [40], and hence the procedure of differential deconvolution is more useful in this regard. From these results we conclude that differential-wavelength deconvolution simplifies the determination of the kinetic constants and fractional intensities for even the more complex reversible two-state reactions.

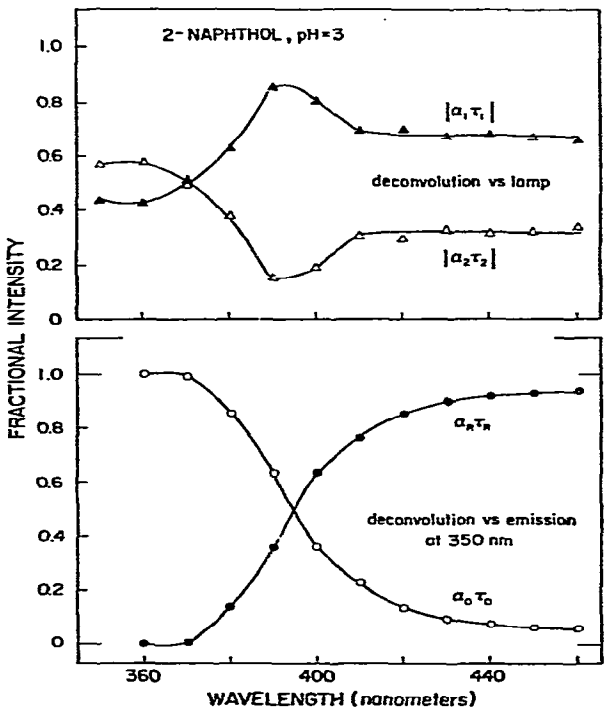

Fig. 9. Fractional intensities of the naphthol and naphtholate emission obtained by differential-wavelength deconvolution. For comparative purposes we also show the values of $|\alpha_i\tau_i|$ obtained by deconvolution versus the lamp pulse.

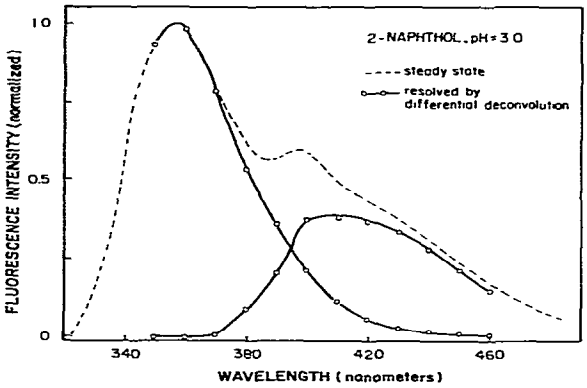

Fig. 10. Resolution of the spectra of naphthol and naphtholate in the presence of a reversible excited-state reaction (pH 3.0).

4.4. Spectral relaxation of PRODAN in n-butanol

As a final example of the application of differential-wavelength deconvolution we examined PRODAN (6-propionyl-2-dimethylaminonaphthalene) in *n*-butanol at −55°C. The fluorescence emission spectrum of PRODAN is highly sensitive to solvent polarity [25] and MacGregor and Weber [26] have speculated that this fluorophore interacts with two or more solvent molecules. We tested this speculation by the use of phase-modulation methods and found that spectral relaxation was indeed a multiple-step process [15]. Here we confirm this result by the use of differential-wavelength deconvolution. Assume that spectral relaxation of PRO-

DAN requires two discrete steps, i.e., a three-state process. In section 2 we demonstrated that by deconvolving the time-resolved emission versus the initially excited state, the expected triple exponential decay of fluorescence is simplified to a doubly exponential decay (eqs. 61–63). When deconvolved versus the exciting pulse a one-step reaction yields a double-exponential decay in which one term has a negative preexponential factor, indicating an excited-state process. Hence, if the time-resolved decay, obtained following deconvolution versus the initially excited state, contains a term with a negative preexponential factor this demonstrates the existence of a state intermediate between the initial and final states. The results of this analysis are listed in table 3. A term with a negative preexponential factor was observed on the long-wavelength side of the emission, irrespective of whether the deconvolution was performed using the exciting pulse or the emission at 400 nm. The nearly equal magnitude and opposite signs of the preexponential factors indicate minimal spectral overlap of the final state with the intermediate or initially excited state [16].

Table 3

Time-resolved decays of PRODAN in *n*-butanol at −55°C

Emission wavelength (nm)	τ_1 (ns)	τ_2 (ns)	$\alpha_1\tau_1$ (%)	χ_2
Deconvolution versus lamp pulse				
400	1.6	0.2	46	1.8
430	1.7	0.1	72	1.3
450	2.7	1.7	41	1.6
470	3.4	–	98	1.9
490	3.4	⟨1.5⟩ [a]	74	2.4
510	3.1	⟨2.4⟩	66	3.0
530	3.4	⟨2.4⟩	60	1.5
550	4.2	⟨1.3⟩	77	3.0
Deconvolution versus 400 nm response				
430	1.3	0.06	28	1.5
450	1.9	0.3	55	1.5
470	2.9	0.5	80	1.7
490	3.2	⟨1.9⟩	85	1.7
510	3.2	⟨2.5⟩	70	4.4
530	5.8	⟨6.3⟩	56	3.1
550	3.4	⟨2.3⟩	61	1.3

[a] The brackets indicate a negative preexponential factor.

We recognize that the assumed model is probably too simple, and that even a three-state model is inadequate to represent accurately the observed decays. This fact is reflected in the larger values for χ^2. Nonetheless, these data indicate that at least two steps are involved in spectral relaxation and illustrate the usefulness of differential-wavelength deconvolution in the analysis of these more complex cases.

5. Discussion

The unambiguous resolution of spectra and kinetic constants using differential-wavelength deconvolution requires one favorable circumstance. This condition is the existence of a region of the emission where only the F state emits. This spectral region is generally found on the short-wavelength side of the emission spectrum. In practice this condition is not very restrictive, and spectral regions of nonoverlap are commonly observed. This condition was satisfied for the reactions studied in this paper. As additional examples of nonoverlap of the F and R states on the blue edge of the spectra we note the following cases: nonoverlap of monomer and exciplex emission was found in polymers of polystyrene [27], for the exciplex between benzophenone and dimethylaniline [28] and is quite generally observed for exciplexes of aromatic hydrocarbons with amines [29–32]. It also appears that nonoverlap regions exist for monomer or excimer fluorescence from pyrene and other aromatic hydrocarbons [3]. Moreover, nonoverlap of the donor spectrum with the acceptor is frequently found in fluorescence energy transfer [5]. Hence, this specific requirement is satisfied for a variety of excited-state reactions which are of general interest.

The simplicity of differential-wavelength deconvolution should facilitate the widespread application of this technique. This deconvolution procedure provides rapid determination of the spectra and kinetic constants which are of interest. When time-resolved data are deconvolved relative to the excitation pulse, the resulting complexity of the

observed parameters hinders interpretation of the data. The difficulties caused by this complexity are well known, especially when more than two excited-state species were present [33–35]. In section 2 we demonstrated that multiple-step irreversible reactions could be analyzed if the nonoverlap condition is satisfied for the appropriate states.

The principle of internal convolution and theory of differential-deconvolution could be also applied to numerous other situations where consecutive reactions occur. Examples include energy transfer among pigments involved in photosynthesis, multiple-step chemical and enzymatic reactions and analysis of individual portions of complex metabolic pathways. Of course, for the latter two cases the nonoverlap requirement is replaced by the need for some other independent quantification. One needs to quantify the amount of the product of interest relative to the amounts of its precursor, a task which has become easier because of advances in analytical instrumentation.

A further advantage of differential-wavelength deconvolution is the minimal need for additional data acquisition and its applicability using existing software. In the analysis of an excited-state reaction using time-resolved methods one generally collects the time profile of the excitation pulse and the responses on the blue and red edges of the emission spectrum. These are precisely the data needed for differential-wavelength deconvolution. These data are analyzed in two different ways, these being the deconvolution of each time-resolved emission with the excitation pulse and then deconvolution of the response at long wavelength with that observed for the shorter-wavelength nonoverlap region. For deconvolution we used the methods of nonlinear least squares [18,19] and modification of the program is not necessary for differential-wavelength deconvolution. We have not used the methods of moments [36] or the Laplace transform methods [31], but it seems likely that similar results would be obtained.

Differential-wavelength deconvolution may also facilitate the determination of similar decay rates when these rates originate from an excited-state process rather than ground-state heterogeneity. It is well known that the determination of such closely spaced decays is difficult. Consider a hypothetical experiment in which the decay times of the F and R states are 2 and 4 ns, respectively, and that the reaction is irreversible. Those experienced with pulse fluorometric methods will recognize that separation of the 2 and 4 ns components present in the emission of the R state could pose some problems. When analyzed by the differential-wavelength deconvolution method the problem is reduced to the determination of a 4 ns lifetime with a relatively wide exciting pulse, this 'pulse' being the F state response. Overlap of the states is revealed as a component with an apparent decay time near zero. Experimentally, it is easier to quantify components with the more disparate decay times (0 and 4 ns) than those with the more similar decay times (2 and 4 ns). It is not unexpected that a differential procedure would provide increased precision.

In another publication we used the increased precision provided by differential-wavelength deconvolution to detect a small percentage of solvent relaxed emission from *N*-acetyl-L-tryptophanamide in vitrified propylene glycol [20]. This capability of differential-wavelength deconvolution may aid in the detection of small spectral components due to relaxed emission from proteins. The existence of such components have been suggested from the wavelength-dependent lifetimes of tryptophan fluorescence from proteins [11,38], and the possible existence of emission from ionized tyrosine residues in proteins [39]. For the cases of dipolar relaxation the two-state model may be inadequate to describe the time-dependent spectral shifts. Nonetheless, differential-wavelength deconvolution may aid the analysis of these more complex cases. The observed response on the blue side of the emission can be assumed to represent the F state and one can use this response to deconvolve the observed response at longer wavelengths. The derived impulse responses will contain a short-lived component which may be assumed to represent the initially excited state. The fractional intensity of this component can be quantified at different emission wavelengths, yielding the emission spectrum of the initially excited state. By difference one obtains the spectrum due to the relaxed state(s). We used this procedure in our resolution of the initially excited and the

solvent relaxed emission spectra of *N*-acetyl-L-tryptophanamide in propylene glycol [20]. The resolution of states obtained by this procedure is arbitrary because solvent relaxation probably proceeds as a multiple-step or continuous process. In addition, the F and R state emission may overlap on the blue side of the emission. Although arbitrary, this procedure was capable of revealing small spectral components formed by solvent relaxation.

In total, favorable circumstances summarized above indicate the general usefulness of differential-wavelength deconvolution in the analysis of excited-state processes. Furthermore, realization of the principle of internal convolution may simplify the analysis of complex kinetic processes.

Acknowledgements

The authors thank Professor Adil E. Shamoo for the use of his pulse fluorometer and acknowledge the Department of the Navy who supplied funds to purchase this instrument. This work was supported by Grant PCM 80-41320 from the National Science Foundation. J.R. L. is an Established Investigator of the American Heart Association. A.B. is on leave from Nicholas Copernicus University, Institute of Physics, Torun, Poland.

References

1 M.G. Badea and L. Brand, Methods Enzymol. 61 (1979) 378.
2 J.R. Lakowicz, J. Biochem. Biophys. Methods 2 (1980) 91.
3 H.J. Galla and W. Hartmann, Chem. Phys. Lipids 27 (1980) 199.
4 J.M. Vanderkooi and J.B. Callis, Biochemistry 13 (1974) 4000.
5 L. Stryer and R.P. Haugland Proc. Natl. Acad. Sci. U.S.A. 58 (1967) 719.
6 D.D. Thomas, W.F. Carlsen and L. Stryer, Proc. Natl. Acad. Sci. U.S.A. 75 (1978) 5746.
7 M.R. Loken, J.W. Hayes, J.R. Gohlke and L. Brand, Biochemistry 11, (1972) 4779.
8 J.H. Easter, R.P. DeToma and L. Brand, Biochim. Biophys. Acta 508 (1979) 27.
9 J.R. Lakowicz and D. Hogen, Biochemistry 20 (1981) 1366.
10 A Gafni, R.P. DeToma, R.F. Marrow and L. Brand, Biophys. J. 17 (1977) 155.
11 J.R. Lakowicz and H. Cherek, J. Biol. Chem. 255 (1980) 831.
12 J.R. Lakowicz and H. Cherek, Biochem. Biophys. Res. Commun. 99 (1981) 1173.
13 H. Morawetz and I.Z. Steinberg, Ann. N.Y. Acad. Sci. 366 (1981).
14 J.R. Lakowicz and A. Balter, Biophys. Chem. 16 (1982) 99.
15 J.R. Lakowicz and A. Balter, Biophys. Chem. 16 (1982) 117.
16 J.R. Laws and L. Brand J. Phys. Chem. 83 (1979) 795.
17 A. Gafni and L. Brand, Chem. Phys. Lett. 58 (1978) 346.
18 W.R. Ware, L.T. Doemeny and T.L. Nemzek, J. Phys. Chem. 77 (1973) 2038.
19 D.V. O'Connor, W.R. Ware and J.C. Andre, J. Phys. Chem. 83 (1979) 1333.
20 J.R. Lakowicz and A. Balter 15 (1982) Biophys. Chem. 353.
21 J.R. Lakowicz and H. Cherek, J. Biochem. Biophys. Methods 5 (1981) 19.
22 N.G. Bakhshiev, Yu.T. Mazurenko and I.V. Piterskaya, Opt. Spectrosc. 21 (1966) 307.
23 W. Rapp, H.H. Klingenberg and H.E. Lessing, Ber. Bunsen-ges. 75 (1971) 883.
24 J.B. Birks, Photophysics of aromatic molecules (Wiley-Interscience, New York, 1970) p. 304.
25 G. Weber and F.J. Farris, Biochemistry 18 (1977) 3075.
26 R.B. MacGregor and G. Weber, Ann. N.Y. Acad. Sci. 366, (1981) 140.
27 T. Ishie, T. Handa and S. Matsunaga, Makromol. Chem. 178 (1977) 2351.
28 H. Masuhara, Y. Maeda, H. Nakajo, N. Matoga, K. Tomita, H. Tatemitsu, Y. Sokota and S. Misumi, J. Am. Chem. Soc. 103 (1981) 634.
29 E.A. Chandross and H.T. Thomas Chem. Phys. Lett. 9 (1971) 393.
30 M.G. Kuzmin and L.N. Guseva, Chem. Phys. Lett. 3 (1969) 71.
31 W.R. Ware and H.P. Richter, J. Chem. Phys. 48 (1968) 1595.
32 H. Knible, D. Rehm and A. Weller, Ber. Bunsenges. 72 (1968) 257.
33 P. Maroti, A. Ringler, G. Laczko and L. Szalay, Acta Phys. Pol. A54 (1978) 789.
34 P.E. Zinsli, J. Photochem. 3 (1974/5) 55.
35 A.J. Roberts, D.V. O'Connor and D. Phillips, Ann. N.Y. Acad. Sci. 366 (1981) 109.
36 I. Isenberg and R.D. Dyson, Biophys. J. 9 (1969) 1337.
37 A. Gafni, R.L. Modlin and L. Brand, Biophys. J. 15 (1975) 263.
38 A. Grinvald and I.Z. Steinberg Biochemistry 13 (1974) 5107.
39 J.W. Longworth Ann. N.Y. Acad. Sci. 366 (1981) 237.
40 S.R. Meech, D.V. O'Connor, A.J. Roberts and D. Phillips, Photochem. Photobiol. 38 (1981) 159.